IL NUOVO CIMENTO **39 C** (2016) 275
DOI 10.1393/ncc/i2016-16275-0

Communications: SIF Congress 2015

Isospin influence on the IMFs production in the ^{78,86}Kr+^{40,48}Ca reactions at 10 AMeV

B. Gnoffo
INFN, Sezione di Catania - Catania, Italy

received 9 February 2016

Summary. — Some results of the analysis of the reactions $^{78,86}\mathrm{Kr} + {}^{40,48}\mathrm{Ca}$ at 10 AMeV are presented. In particular the neutron enrichment effects on the production mechanisms of the Intermediate Mass Fragments are investigated. The reaction products show different isotopic composition and relative richness between the two systems. An odd-even staggering effect is present in the charge distributions of the reaction products, in particular for the light fragments produced by the neutron-poor system. The kinematical characteristics of the IMFs indicate a high degree of relaxation of the degrees of freedom of the formed systems, indicating a production by equilibrated fission-like process.

1. – Introduction

Heavy-ion collisions are characterized by reaction mechanisms that lead to the formation of fragments in a wide mass range. In the last years the problem of identifying the production sources of fragments with an atomic number $3 \leq Z \leq 20$, denoted as Intermediate Mass Fragments, IMFs, has attracted particular attention. This is because this production reflects the interplay between statistical properties of highly excited nuclei and fission process. In the intermediate energy domain ($15\,\mathrm{MeV} \leq E/A \leq 100\,\mathrm{MeV}$) an abundant IMFs production is observed [1, 2], especially by increasing the reaction inelasticity; because of the broad velocity distribution, from the target-like fragments (TLF) up to the projectile-like (PLF) fragments, both statistical and dynamical mechanisms (target or projectile fission, neck emission and multifragmentation) seem to be responsible of the IMFs production.

The reactions in the low-energy regime are dominated by the competition between binary process (DIC, quasi-fission) and the compound nucleus de-excitations. These decay channels have precise kinematical characteristics that allow to identify the IMFs emission process.

The IMF production is influenced by many features of the entrance channel, in particular, the neutron richness plays an important role. In fact, as is well known in the literature [3-5], the even-odd effect, the staggering, observed in the charge distribution, decreases with the enhancement of the N/Z ratio.

In the present paper the kinematical inclusive analysis of the IMFs production processes in the reactions ^{78}Kr + ^{40}Ca and ^{86}Kr + ^{48}Ca at 10 AMeV is discussed.

Angular distributions and the features of the emission velocities suggest a preferential IMFs production via an asymmetric binary equilibrated process following a compound nucleus formation.

Isotopic composition shows that some memory of the entrance channel is still present in the exit channel.

The production cross sections are compared to the theoretical prediction of the statistical model Gemini++. An important feature of this model is that it does not take into account only the dominant decay modes, fusion, evaporation and fission, but it includes also the IMFs emission.

2. – Experimental set up

The experiment, called ISODEC [6, 7], was performed at the INFN Laboratori Nazionali del Sud (LNS) in Catania by using beams of ^{78}Kr and ^{86}K, delivered at 10 AMeV by the Superconductive Cyclotron and with a typical intensity of 800–1000 pA and a timing resolution of about 800 ps–1 ns.

In the experiment, self-supporting 1 mg/cm^2 thick ^{40}Ca and ^{48}Ca targets, prepared in collaboration between INFN-LNL and INFN-LNS Target Laboratories, were used.

For the detections of the reaction products, the second-generation 4π multidetector CHIMERA [8] for charge particle was used.

The CHIMERA device consists of 1192 detector telescopes; 688 are arranged on 9 rings in the forward part, that cover a polar angle from $\theta = 1°$ to $\theta = 30°$, while the other 504 telescopes are arranged in the backward part on 17 rings in spherical configuration, that cover from $\theta = 30°$ to $\theta = 176°$. The efficiency is 94% of the total solid angle.

Each module consists of a silicon detector (Si, thickness about 300 μm) followed by a caesium iodine thallium doped crystal (CsI(Tl), thickness from 3 cm to 12 cm), coupled to a photodiode. Different identification methods can be used [9]:

- ΔE-E for charge identification of particles punching through the Si detector and stopped in the CsI(Tl) with also mass identification for ions with $Z \leq 10$;
- E-TOF (Time of Flight) for direct velocity measurement of all the reaction products and for the mass identification of the particles stopped in the Si detector;
- PSD (Pulse Shape Discrimination) in CsI(Tl), for isotopic identification of more energetic light particles;
- PSD (Pulse Shape Discrimination) in silicon, for charge identification of the particles stopped in this detector.

This latter identification technique (PSD in silicon detector) recently implemented on the CHIMERA array, was fundamental for the realization of the ISODEC experiment because it allows the use of this device to study reaction mechanisms also in the low energy domain, extending the investigation dynamical range of the detector from multifragmentation to fusion reactions.

In fig. 1 is reported an example of the typical Energy *vs.* Rise-Time plot obtained for the n-poor system, ^{78}Kr + ^{40}Ca, at $\theta = 34°$ and used for the charge identification through the PSD method in silicon.

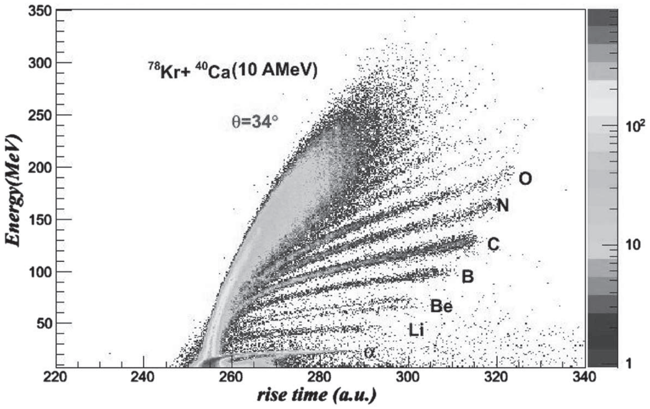

Fig. 1. – Energy *vs.* rise-time plot for the ^{78}Kr + ^{40}Ca reaction at $\theta = 34°$.

3. – Experimental results

In order to identify the mechanisms responsible of the IMFs production, an analysis of the kinematical characteristics was performed. The time of flight technique allows good measurement of the velocity spectra providing precise average values of the velocities. The results obtained in the center-of-mass frame, at different laboratory angles are plotted, for the n-poor system, in fig. 2 for Z from 3 up to 17. The quasi-linear decrease of the mean values of the velocities in the center-of-mass frame with increasing atomic number and the independence of these values from the emission angles suggest a high relaxation of all degrees of freedom in the production mechanisms [3, 10, 11].

Moreover the mean values of the velocities, in the center-of-mass frame, averaged over all laboratory angles, are well reproduced by the theoretical prediction of Viola's

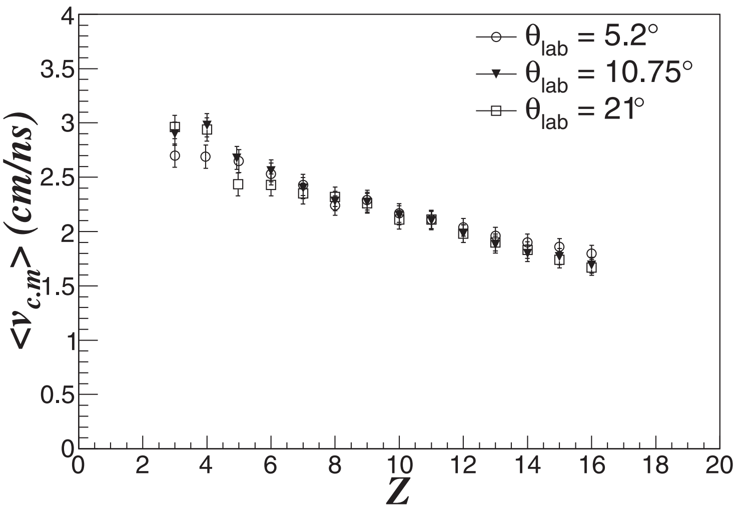

Fig. 2. – Values of the average velocities, in the center-of-mass frame, *vs.* the atomic number at three different laboratory angles for the ^{78}Kr + ^{40}Ca at 10 AMeV.

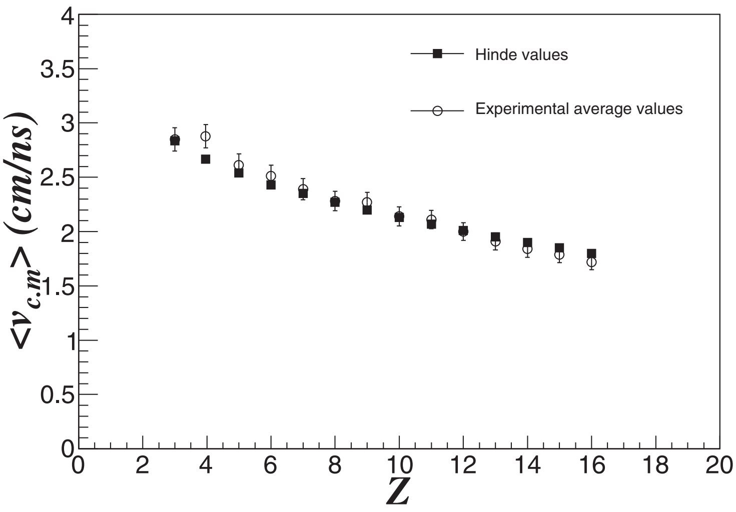

Fig. 3. – For the ^{78}Kr + ^{40}Ca: Comparison of the mean values of the velocity, in the center-of-mass frame, averaged over all angles, with the values of Hinde's systematic.

systematic with the corrections by Hinde [12] for the asymmetric fission as it is shown in fig. 3. Viola's systematic provides the most probable energy released in the statistical fission process [13].

All these kinematical features lead to identify the production mechanism of IMFs with an asymmetric binary fission following compound nucleus formation. This is confirmed by a $1/\sin\theta_{c.m.}$ trend (solid line in the picture) of the IMFs angular distributions in the center-of-mass frame, shown in fig. 4. This behavior, expected for a production via a

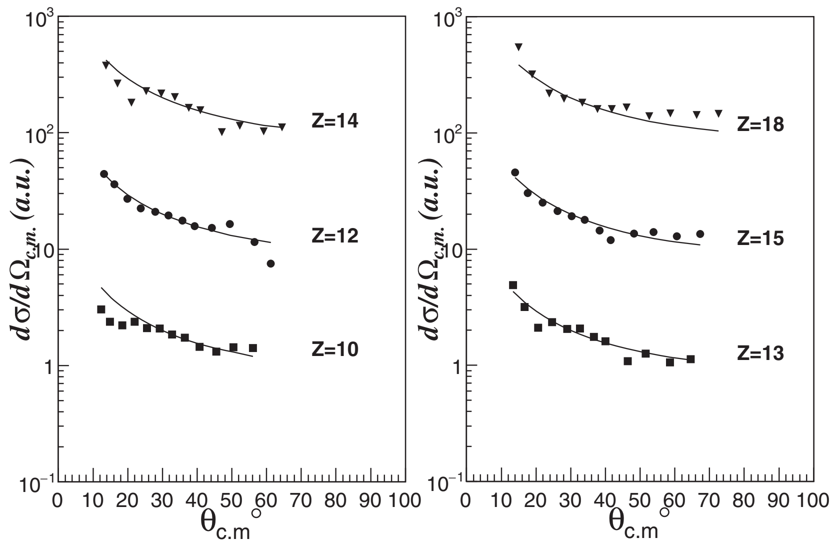

Fig. 4. – For the ^{78}Kr + ^{40}Ca reaction: Angular distributions of IMFs, in the center-of-mass frame, compared to $1/\sin\theta_{c.m.}$ (solid line). The error bars are inside the graphical symbol.

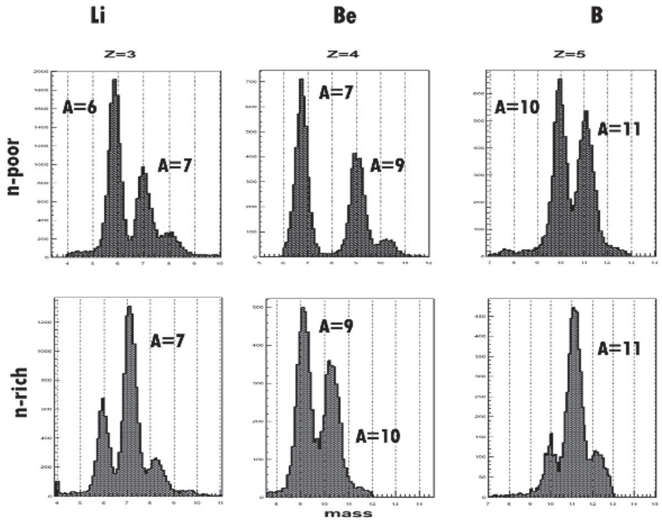

Fig. 5. – Isotopic composition of $Z = 3, 4, 5$ fragments (bottom panels for the n-rich system, top panels for the n-poor one).

long-lived system with a lifetime comparable to its rotational period, that implies a loss of the memory of the entrance channel, is in opposition to fast processes that show a preferential emission direction [14]. The results discussed until now were shown for the n-poor system but similar considerations can be made for the n-rich one.

The production of the emitted fragments is influenced by the isospin degree of freedom. Deep differences between the two studied systems are observed in the isotopic composition and relative abundance, presented in fig. 5, and in the charge distributions of the reaction products. In general the n-rich system prefers to produce the heavier isotopes of the same element compared to n-poor system showing some persistence of the memory of entrance channel in the exit channel. In particular this effect is more evident for the Beryllium element, in which the isotopic composition goes from ^{7,9}Be in the ^{78}Kr + ^{40}Ca reaction up to ^{9,10}Be in the ^{86}Kr + ^{48}Ca.

The total IMFs production cross section was obtained by integrating the inclusive angular distributions, assumed to follow a $1/\sin\theta_{c.m.}$ trend. The differential cross sections $\mathrm{d}\sigma/\mathrm{d}\Omega$ were normalized with respect to the elastic scattering, choosing for the normalization a detector that covers the polar angle range $\theta_{lab} = 1.8°–2.4°$. The results are shown in fig. 6.

A probable underestimation of the Be yields is observed because of the missed ^{8}Be direct detection due to the short lifetime. In order to correct the Be cross sections the study of the coincidence of two alphas emitted in the same detector, in general the CHIMERA detectors cover angles greater than those between two alphas emitted in ^{8}Be decay, is necessary. The depression of the Be yields seems to be greater for the n-poor system, probably because, as mentioned earlier, in the reaction ^{86}Kr + ^{48}Ca there is a preferential emission of the heavier beryllium isotopes.

A strong even-odd effect, the staggering, is observed in the charge distributions of the fragments produced, shown in fig. 6 where the fragments yields are plotted as functions of their charge. This effect is due to a preferential production of fragments with an even value of the atomic number, because of the greater stability, consequence of a larger binding energy.

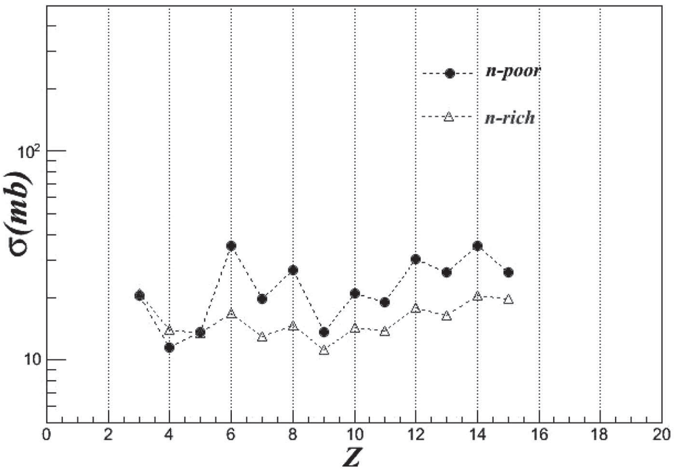

Fig. 6. – Production cross section for fragments with different atomic numbers for the two reactions ^{78}Kr + ^{40}Ca and ^{86}Kr + ^{48}Ca. The error bars are inside the graphical symbols.

In agreement with other examples in the literature the staggering is more pronounced for the n-poor system compared to the n-rich one, in particular for $Z < 10$ reaction products. This effect persists for higher Z with a smaller amplitude. The IMFs production is favored in the ^{78}Kr + ^{40}Ca reaction, in fact the cross sections are systematically higher. The neutron enrichment seems to affect the cross sections of the lighter IMFs, but an influence can also arise from structure effects, linked to the pairing force, that could be connected to the symmetry energy [15].

The production cross sections were compared to theoretical predictions of the GEMINI ++ model, the results are shown in fig. 7. This model, developed by R. Charity, combines

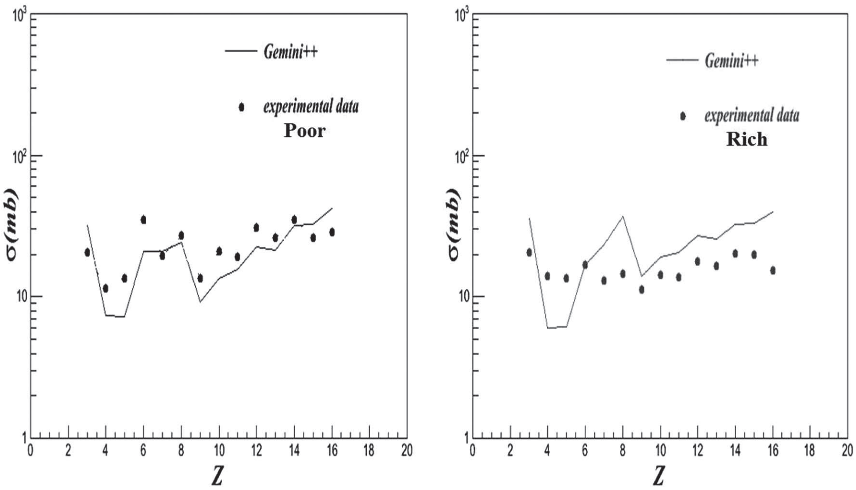

Fig. 7. – The cross section for fragments production for the ^{78}Kr + ^{40}Ca (left panel) and for ^{86}Kr + ^{48}Ca (right panel) are shown as a function of the atomic number Z. The present data are compared with model predictions obtained with the code GEMINI ++.

the Hauser-Feshbach [16] evaporation formalism with binary decay formalism in order to describe the emission, by the compound nucleus, of fragments in a wide range of mass, from evaporated particles up to the symmetric fission fragments.

The Gemini ++ code describes the IMFs production through the Moretto binary decay model [17], an extension of the Bohr-Wheeler transition state formalism [18] to the asymmetric fission.

The model is able to reproduce slightly better the distribution relative to an n-poor system. The staggering is well reproduced and in agreement with the experimental data, the oscillation amplitude decreases with increasing the atomic number. The yields are underestimated, probably because the model undervalues secondary emissions, but to check that primary products are actually emitted with an excitation energy sufficient to further decays, a study of IMFs and Light Charge Particles coincidences will be performed.

On the contrary the Gemini ++ model fails to reproduce the experimental distribution relative to ^{86}Kr + ^{48}Ca reaction, probably because the neutron richness introduces some ingredients concerning the IMFs production that the model does not take into account.

4. – Conclusions

The features of the IMFs production mechanisms in reactions ^{78}Kr + ^{40}Ca and ^{86}Kr + ^{48}Ca at 10 AMeV suggest a high relaxation of the degrees of freedom of the system formed in the collisions before the breakup. In fact the mean value of the c.m. velocities, almost independent of the emission angles and the angular distributions well fitted by $1/\sin\theta_{c.m.}$ are evidences of preferential IMFs emission by a typical fusion-fission–like reaction mechanism.

The isospin strongly influences the characteristics of IMFs emission; significant differences between the two studied systems are observed in the isotopic composition and relative abundance.

The charge distributions show an even-odd staggering effect that is more pronounced for the n-poor system, in particular for fragments with atomic number $Z < 10$, the staggering is still present for the other fragments but with a low oscillation amplitude.

The comparison with GEMINI++ model shows a better agreement with the experimental charge distribution of the ^{78}Kr + ^{40}Ca reaction.

Data analyses are in progress. Important information will be obtained from the study of the Light Charge Particles and IMF coincidences.

Comparisons with dynamical models [19], as well as statistical models, are necessary to provide indications about the isospin influence on the competition between different modes of the IMFs formation.

In order to study the evolution, with isospin asymmetry, of the reaction dynamics and to investigate the interplay between the nuclear structure and reaction mechanism a Letter Of Intent was presented at the "Second SPES International Workshop at INFN-LNL" to study the reactions ^{92}Kr + ^{40,48}Ca at 10 AMeV by using a neutron rich radioactive beam.

* * *

The author would like to especially thank Dr. S. Pirrone and Prof. G. Politi for useful exchanges concerning the analysis and precious scientific support. Prof. J. P. Wieleczko and the whole INFN-CHIMERA-NEWCHIM collaboration, in particular E. De Filippo, P. Russotto and M. Trimarchi, are gratefully acknowledged.

REFERENCES

[1] Peilert G., Stocker H. and Greiner W., *Rep. Prog. Phys.*, **57** (1994) 6.
[2] De Filippo E. and Pagano A., *Eur. Phys. J. A*, **50** (2014) 32.
[3] Ademard G. *et al.*, *Phys. Rev. C*, **83** (2011) 054619.
[4] Lombardo I. *et al.*, *Phys. Rev. C*, **84** (2011) 024613.
[5] Casini G. *et al.*, *Phys. Rev. C*, **86** (2012) 011602.
[6] Pirrone S. *et al.*, *J. Phys. Conf.*, **515** (2014) 012018.
[7] Politi G. *et al.*, *JPS: Conf. Proc.*, **6** (2015) 030082.
[8] Pagano A. *et al.*, *Nucl. Phys. News*, **22** (2012) 25.
[9] Politi G. *et al.*, *IEEE NSS: Conf. Rec.* (2005) N28-5.
[10] Charity R. J. *et al.*, *Nucl. Phys. A*, **476** (1988) 516.
[11] Jing K. X. *et al.*, *Nucl. Phys. A*, **645** (1999) 203.
[12] Hinde D. J. *et al.*, *Nucl. Phys. A*, **472** (1987) 318.
[13] Viola V. E. *et al.*, *Phys. Rev. C*, **31** (1985) 1550.
[14] Hinde D. J. *et al.*, *Phys. Rev. C*, **60** (1999) 054602.
[15] D' Agostino M. *et al.*, *Nucl. Phys. A*, **861** (2011) 47.
[16] Hauser W. and Feshbach H., *Phys. Rev.*, **87** (1952) 366.
[17] Moretto L. G. *et al.*, *Nucl. Phys. A*, **247** (1975) 211.
[18] Bohr N. and Wheeler J. A., *Nucl. Phys. A*, **56** (1939) 426.
[19] Kalandarov S. A. *et al.*, *Phys. Rev. C*, **82** (2010) 044603.